

## Material migration and erosion of plasma-facing components in the full-tungsten WEST tokamak during its Phase 1 and Phase 2 operations

A. Hakola<sup>1</sup>, M. Diez<sup>2</sup>, E. Bernard<sup>2</sup>, S. Di Genova<sup>2</sup>, A. Huart<sup>2</sup>, N. Fedorczak<sup>2</sup>, J. Gaspar<sup>3</sup>, E. Tsiatroni<sup>2</sup>, Y. Corre<sup>2</sup>, K. Krieger<sup>4</sup>, A. Widdowson<sup>5</sup>, M. Balden<sup>4</sup>, I. Bogdanovic Radovic<sup>6</sup>, E. Fortuna-Zalesna<sup>7</sup>, E. Grigore<sup>8</sup>, I. Jögi<sup>9</sup>, M. Kelemen<sup>10</sup>, A. Lagoyannis<sup>11</sup>, J. Likonen<sup>1</sup>, S. Markelj<sup>10</sup>, C. Martin<sup>3</sup>, R. Mateus<sup>12</sup>, K. Mergia<sup>11</sup>, P. Paris<sup>9</sup>, P. Petersson<sup>13</sup>, Z. Siketic<sup>6</sup>, P. Tsavalas<sup>11</sup>, T. Vuoriheimo<sup>14</sup>, WEST team\*, EUROfusion Tokamak Exploitation Team\*\*

<sup>1</sup>VTT, Espoo, Finland; <sup>2</sup>CEA, IRFM, Saint-Paul-Lez-Durance, France; <sup>3</sup>Aix Marseille University, Marseille, France; <sup>4</sup>Max-Planck-Institut für Plasmaphysik, Garching, Germany; <sup>5</sup>UKAEA, Culham Science Centre, Abingdon, UK; <sup>6</sup>Ruder Bošković Institute, Zagreb, Croatia; <sup>7</sup>Warsaw University of Technology, Warsaw, Poland; <sup>8</sup>National Institute for Laser, Plasma and Radiation Physics, Bucharest, Romania; <sup>9</sup>University of Tartu, Tartu, Estonia; <sup>10</sup>Jožef Stefan Institute, Ljubljana, Slovenia; <sup>11</sup>National Centre for Scientific Research "Demokritos", Athens, Greece; <sup>12</sup>Instituto Superior Técnico, Bobadela, Portugal; <sup>13</sup>KTH Royal Institute of Technology, Stockholm, Sweden; <sup>14</sup>University of Helsinki, Helsinki, Finland; \*See <http://west.cea.fr/WESTteam>; \*\* E. Joffrin et al. 2024 Nucl. Fusion **64** 112019

Email: [antti.hakola@vtt.fi](mailto:antti.hakola@vtt.fi)

Tungsten (W) is the primary candidate material for the plasma-facing components (PFCs) in future fusion reactors. WEST is a full-W tokamak with long-pulse capabilities and therefore an ideal testbed for studying erosion and subsequent migration of W in the scrape-off layer (SOL) plasma under varying operational conditions and with different PFC geometries. In this contribution, we will report the results of extensive efforts within the EUROfusion programme to obtain a global picture of material migration pathways during the Phase 1 (2016-2021, mix of passively-cooled W-coated graphite and actively-cooled bulk W divertor PFCs) and Phase 2 (from 2022 onwards, full actively-cooled divertor with ITER-grade monoblock structures) operational phases of WEST. The focus is at the divertor region, where the database is the most extensive. *Gross erosion*, i.e., primary sputtering of W is determined via spectroscopic techniques while for *net-erosion* investigations, to take (prompt) *re-deposition* of W into account, selected PFCs are removed from the vessel for *post mortem* surface analyses in the participating laboratories.

### Material migration during Phase 1 operations

The determined gross-erosion rates of W during Phase 1 are in line with published data from other tokamaks with full or partial W coverage, of the order of 1-2 nm/s in L-mode plasmas [1,2]. Sputtering is largely dominated by impurities such as boron (B), carbon (C), nitrogen (N), oxygen (O), and neon (Ne). The strongest W erosion flux is observed at the divertor while the sources in the main chamber are weaker but poorly screened, thus setting strong requirements for controlling impurity transport into the core. Another WEST-specific observation is a notable asymmetry in the W gross erosion between the low-field-side (outer) and high-field-side (inner) divertor targets: in L-mode sputtering can be a factor of 2-5 higher on the inner side [2]. The reason can be associated with the complex interplay between the plasma conditions and the impurity profiles responsible for W erosion at the WEST divertor. Comparison between deuterium (D) and helium (He) plasmas shows that gross erosion is more intense in He but even more importantly, radiative losses in the plasma become more intense and W sources are extinguished at higher densities in He than in D.

Net-erosion studies rely largely on surface analyses of special *marker PFCs*, removed from the divertor after completing the C3 (2018), C4 (2019), and C5 (2020) experimental campaigns on WEST [3], Fig. 1. All the marker tiles exhibit W (1-2  $\mu\text{m}$ ) coatings with molybdenum (Mo) interlayers ( $\sim 0.1 \mu\text{m}$ ) on top of the standard W-coated graphite PFCs. In addition, a set of ITER-like divertor plasma-facing units (PFUs) consisting of W monoblocks (MB) with an unshaped flat-top geometry were analysed [3]. Distinct net-erosion regions are observed both at the inner and outer *strike-point* areas with the most pronounced features close to the outer strike point. The net-erosion rates typically are in the range 0.1-0.5 nm/s, in agreement with data from ASDEX Upgrade (AUG) [4]. The areas dominated by net erosion become more extended in the poloidal direction from campaign to campaign, with the largest changes occurring between C3 and C4. In addition, a poloidal shift of the main erosion peaks towards the SOL region on both divertor targets is observed. Notable deposited layers with thicknesses up to 50  $\mu\text{m}$  are measured on the divertor, especially on the inner divertor SOL adjacent to the strike point [3,5] as well as a narrow poloidal region where net erosion turns into net deposition. The thickest layers show complex morphologies with a stratified structure and significant fractions of B, C, D, and O embedded. Further into the SOL, both on the inner and outer side, thinner ( $< 0.5 \mu\text{m}$ ) deposited layers can

be identified almost independent of the exposure campaign. A dedicated He campaign [6] at the end of C4 resulted in noticeable He inventories (5-10 at.%) close to the inner and outer strike points. In the toroidal direction, especially the net-erosion patterns appear to follow the modulation of the strong magnetic ripple of WEST, with most eroded areas (by an order of magnitude) found in the high-flux zones [7].

### Impact of long pulses and high fluences on material migration during Phase 2 operations

In Phase 2, experimental activities focused on assessing erosion and deposition of W during long pulses and at high fluences. The most striking observation is that the inner-outer asymmetry in gross erosion is even more amplified compared to Phase 1 – a factor of  $\sim 10$  between inner and outer divertor [8]. The thickest deposits are also observed at the inner divertor. Most detailed analyses have been performed after a *high-fluence campaign* in 2023 where the application of repetitive long L-mode pulses in attached divertor conditions in D resulted in an accumulated fluence of  $\sim 5 \times 10^{26} \text{ m}^{-2}$  at the outer strike point. The gross erosion rates were measured to peak to 1-2 nm/s while the deposited layers exhibited thicknesses up to tens of  $\mu\text{m}$  [8] – both in line with the values obtained during Phase 1 (Fig. 1). The structure of the thickest deposits was not drastically different from earlier observations, either: A mixture of low-Z and high-Z elements and signs of melting and delamination. However, a new class of foil-like layers was observed in shadowed areas, with a tendency to become easily delaminated when exposed to air [9]. Fig. 2 shows a photograph and an example of the structure of the thick deposits on the PFU MB surfaces after the high-fluence campaign.

### Modelling material migration on WEST

Tungsten erosion and migration in WEST plasmas has been modelled by SOLEDGE2D/3X and ERO2.0 codes as well as with the help of Particle-In-Cell (PIC) simulations [10] to further elucidate the contributions of the various W sources in the divertor and the main chamber regions. The overall erosion-deposition pattern during Phase 1 can be reproduced using oxygen as a proxy for the overall impurities except for the strong inner-outer asymmetry and the accumulation of thick deposits on the inner divertor surfaces; These can be attributed to the role of SOL flows and drifts similarly to the corresponding studies on AUG [11]. Modelling also tends to underestimate the net-erosion rate, but the results are very sensitive to the applied assumptions as well as the surface morphology. Accounting for the 3D structure of erosion and sputtering from B and N impurities are subjects of ongoing modelling research.

In conclusion, net erosion of W PFCs during a typical WEST experimental campaign does not present insurmountable issues for the lifetime of divertor components when scaling up to future devices. However, the formation of thick, co-deposited layers is observed on the divertor surfaces during high fluences and long repetitive pulses up to the point where they are prone to flaking and creating UFO events in the plasma. A full explanation for their origin is needed for extrapolations to ITER.

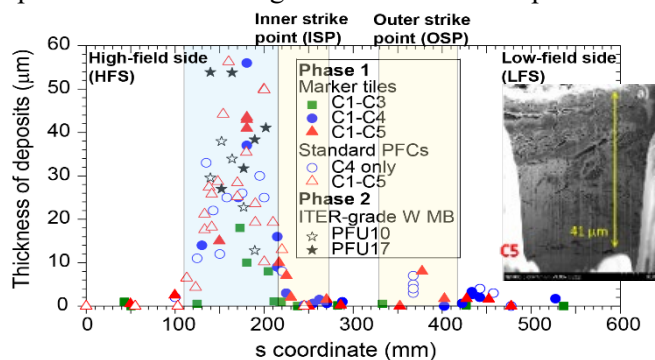


Figure 1. Poloidal profile of the thickness of deposits during Phases 1 and 2 along a divertor component. Inset shows an example of the structure of the thick deposits during Phase 1. Net erosion zones are indicated in yellow, thick deposited layers in blue.

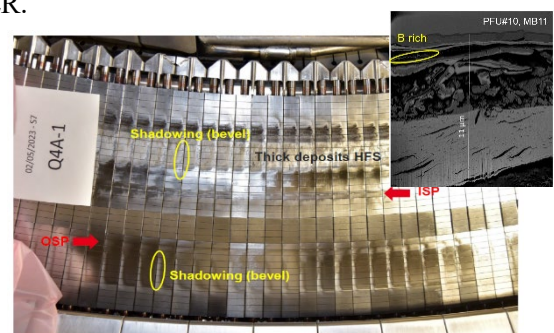


Figure 2. Photograph of a divertor sector removed after the high-fluence campaign in Phase 2. Inset shows the structure of a typical thick deposit. Areas shadowed by the monoblock bevel, where thin foil deposits were observed, are indicated.

- [1] G. J. van Rooij et al., Phys. Scr. **T171** (2020) 014060; [2] C. C. Klepper et al., Plasma Phys. Control. Fusion **64** (2022) 104008; [3] M. Diez et al., Nucl. Mater. Energy **34** (2023) 101399; [4] A. Hakola et al., Nucl. Fusion **61** (2021) 116006; [5] M. Balden et al., Phys. Scr. **96** (2021) 124020; [6] E. Tsiatroni et al., Nucl. Fusion **62** (2022) 076028; [7] M. Balden et al., PFMC 2025 conference (submitted); [8] N. Fedorczyk et al., Nucl. Mater. Energy **41** (2024) 101758; [9] E. Tsiatroni et al., PSI 2024 conference; [10] S. Di Genova et al., Nucl. Fusion **64** (2024) 126049; [11] A. Hakola et al., Nucl. Mater. Energy **25** (2020) 100863